Proc. 5th Int. Topical Meeting on Nuclear Reactor Thermal Hydraulics (NURETH-5),
Salt Lake City, USA. Sept. 21-24, 1992, Vol. II, pp. 358 - 365, Am. Nucl. Soc., LaGrange Park, Ill.

ANALYSIS OF SECOND ORDER TRANSPORT EQUATIONS BY NUMERICAL SIMULATIONS OF TURBULENT CONVECTION IN LIQUID METALS

G. Grötzbach, M. Wörner
Kernforschungszentrum Karlsruhe GmbH, Institut für Reaktorsicherheit
Postfach 3640, 7500 Karlsruhe, Federal Republic of Germany, Fax 07247 823718

ABSTRACT

The method of direct numerical simulation is used to provide a data base for turbulent Rayleigh-Bénard convection in air and sodium at small but comparable Grashof numbers. The results are analysed regarding the similarity of the small scale structures in the velocity fields of both fluids. The data base is also used to calculate some analytical terms of the k and g equations and of corresponding model assumptions used in a standard k-ε-g model. The resulting model coefficients indicate that such standard models need methodological extensions to be applicable to pure natural convection in liquid metals at least at moderate Rayleigh numbers.

INTRODUCTION

There is intensive work going on to analyse the heat transfer capabilities of natural convection in new designs of liquid metal cooled fast breeder reactors [1,2]. The experimental results from scaled reactor models using water as a model fluid will mainly be transfered to reactor conditions by computer codes [3,4]. The turbulence models used for this purpose are going to be improved to be applicable to heat transfer in purely buoyant flows [5,6] and to mixed convection in liquid metals [7]. Data are required to improve model assumptions and to calibrate models for use with pure natural convection in liquid metals. Due to the extreme experimental deficiencies in working with liquid metals only very few suitable data are available [7,8]. Thus, there is a good chance for the method of direct numerical simulation of turbulence [9] to provide such data for at least small turbulence levels.

In this paper we consider the Rayleigh-Bénard convection, that is an infinite horizontal fluid layer heated at the lower wall and cooled at the upper wall. Results from two numerical simulations, for air and sodium at small but comparable Grashof numbers, will be presented and analysed. They will be used to show some peculiar features of turbulence in liquid metals, to predict some terms in the equations for the kinetic energy k and for the temperature variance g, and to analyse in a first step some coefficients of the standard k-ε and the k-ε-g model, especially those used in heat transfer models.

SIMULATION MODEL

The method of direct numerical simulation of turbulence is based on the full mass conservation, Navier-Stokes, and thermal energy equations. The features of turbulence require to solve these equations in three dimensions and in time, and to use grids which resolve the largest and smallest scales of turbulence. When these requirements are met, no assumptions for the subgrid scales and no wall models are needed. Here the grids are chosen to record all relevant flow structures. Thus, the simulations do not depend on any model coefficients.

The simulation model used is the TURBIT code [9]. It is based on the complete three-dimensional time-dependent conservation equations for mass, momentum, and thermal energy. The validity of the Boussinesq approximation is assumed. For normalization we use the channel height D, velocity $u_o = (g\ \beta\ \Delta T_w\ D)^{1/2}$, time D/u_o, and temperature difference ΔT_w, where g = gravity, β = volume expansion coefficient, ΔT_w = temperature difference between the hot lower wall and the cold upper wall, D = channel height. The resulting equations are solved in terms of mesh cell surface averaged velocities $\overline{u_i}$ and volume averaged pressure $\overline{P}$ and temperature $\overline{T}$ by use of a finite difference scheme on a staggered grid. The code was recently extended by a semi-implicit time-integration scheme for the thermal energy equation to improve considerably the efficiency with simulations of liquid metal convection [10]. The momentum equations are solved explicitly. The Poisson equation for the pressure is solved by a direct pseudo-spectral method.

The code was verified by applications to a large number of different flows [9], including the Rayleigh-Bénard convection of air used here for comparison [11] and blind predictions for a benchmark with natural convection of a liquid metal in a rectangular box [10, 12]. Of course there appear no serious problems with direct simulations except for the fact that the user of the code has to know how to specify grids which are adequate to the considered physical problem.

CASE SPECIFICATIONS

The Rayleigh-Bénard convection is characterised by the Rayleigh number $Ra = g \beta \Delta T_w D^3/(va)$ and the Prandtl number $Pr = v/a$ (where v = viscous diffusivity, a = thermal diffusivity). Two simulations are compared here, Tab. 1. The simulation for air, Pr = 0.71, with $Ra = 220 \cdot Ra_{cr}$ is in the fully turbulent regime, the one for sodium, Pr = 0.006, with $Ra = 3.5 \cdot Ra_{cr}$ is also expected to be turbulent in the velocity field [13,14].

Tab. 1: Parameters and grid data for both simulations (i = 1,2).

Pr	Ra	Gr	X_i	Δx_i	Δx_{3w}	N_i	N_3
0.71	$3.8 \cdot 10^5$	$5.4 \cdot 10^5$	7.92	0.044	0.005	180	32
0.006	$6 \cdot 10^3$	10^6	8.0	0.04	0.01	200	31

The grids have to meet two important criteria: The grid widths Δx_i, i = 1,2 horizontal, i = 3 vertical, have to be fine enough to resolve the smallest scales of turbulence and to resolve adequately the thin boundary layers. The horizontal extension X_i of the control volume has to be large enough to avoid hindering of large scale structures as periodic boundary conditions are used in both horizontal directions.

For the simulation with air sufficient experience is available to specify adequate grids [11]. It was shown in [13] that the grid specified for air, Tab. 1, is surely fine enough for simulation purposes, it could be finer for analysing purposes, and that such large periodicity lengths X_i are absolutely necessary to allow for the development of realistic large scale structures.

For the simulation with sodium there is only negligible experience to specify grids. From some physical arguments and a sensitivity study, see below, we deduced a grid which is a bit finer than the one for air for a channel which is a bit larger, Tab. 1. The numbers of mesh cells N_i follow directly from the values chosen for X_i and Δx_i, except for the vertical direction in which non-equidistant grids are used.

The simulations are started from zero velocities and from approximated vertical mean temperature profiles on which random fluctuations are superimposed. To save computing time, the sodium case was run up to $t_{max} = 960$ on a coarser grid using $160^2 \cdot 25$ nodes. The final 3d results were interpolated to the finer grid. The time needed to find again fully developed flow even in the high frequency range of the spectra was about one time unit.

RESULTS

The complete three-dimensional results for the three velocity components, pressure, and temperature are stored for a certain number of time steps. To obtain reasonable statistical data from the time dependent results, averages $\bar{y}$ for a calculated variable y are formed over horizontal planes, and these are averaged over N_{tav} time steps distributed within the period Δt_{av} at the end of the simulated problem time t_{max}, see Table 2. It is this averaging over all points in each horizontal plane which improves strongly the statistical results and which allows to use much smaller sampling times than known from analysing experimental data.

Tab. 2: Problem time simulated and time interval used for time averaging

Pr	t_{max}	Δt_{av}	N_{tav}
0.71	107.2	32.9	11
0.006	995.9	31.2	9

Verification

The simulation for air is one of a series which has been verified extensively by comparison to experimental results [11,13]. The simulation for sodium can not be verified to the same extent because there are only very few suitable experimental data available. The calculated Nusselt number of 1.05 compares roughly with the experiments of Kek [8], which give for all small Rayleigh numbers about 1.10 ± 0.03. This result is not very relevant because it shows that most heat is transfered by conduction, not by convection. A more important comparison can be performed by using the only second type of

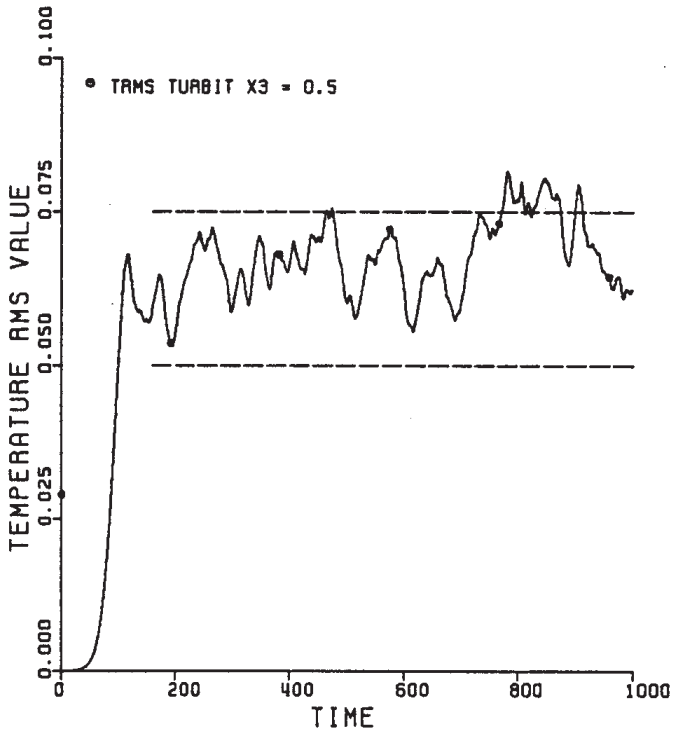

Figure 1. Time trace of $(\overline{T'^2})^{1/2}$ averaged over horizontal mid-plane and error band of data by Kek [8]; Pr = 0.006.

data available at this Rayleigh number from Kek: The time trace of horizontally averaged rms-value of the temperature fluctuations is for t beyond 100 well within the error band of his experimental data, Fig. 1. In addition we should show that none of the computational parameters, like Δx_i, X_i or t_{max}, has a considerable effect on the results.

The influence of Δx_i, that is of the resolution of fine scales, was investigated by five simulations using $80^2 \cdot 13$ up to $200^2 \cdot 31$ mesh cells for a fix channel size of $X_i = 8$. There is a systematic increase in the simulated fluctuation amplitudes, e.g. in the kinetic energy of turbulence, which vanishes for grids using more than about $120^2 \cdot 19$ to $160^2 \cdot 25$ mesh cells. Nevertheless, we used the finest grid mainly because of analysing purposes. The corresponding grid widths found on this way to be required for the simulation with sodium are comparable to those required for the simulation with air. Indeed, vertical cuts through the instantaneous velocity fields at any time and place show for both simulations very similar structures at small scales, e.g. thin shear layers, Fig. 2. Thus these results agree with conclusions from dimensional anaylsis that in natural convection in liquid metals the velocity field is governed by convection. Therefore very small scales exist and the velocity fields are comparable for comparable Grashof numbers, Gr = Ra/Pr. Here the Grashof numbers are of the same magnitude, Tab. 1.

The influence of X_i, that is the capability to resolve large scale structures, was investigated by simulations on a coarse grid using X_i = 4, 6, 8, 10 and 16. The four larger channels allow for development of irregular roll-like structures with horizontal axes. Analysis of the wavelength λ of the irregular rolls results in values for λ of about 2.6 to 2.8. As expected this is larger than the theoretical value λ_{cr} = 2 at the onset of convection [14]. On the other hand it is smaller than the value found in the air flow [13], which is about 3.4, despite the strong thermal conductivity which allows for strong coupling over large distances. Indeed, the temperature field for air shows small spatial structures comparable to those in the velocity fields, whereas the temperature field for sodium is very smooth and shows only weak influences of convection, Fig. 2. Due to the large thermal diffusivity of sodium it is dominated by conduction. A careful statistical analysis shows systematic influences of X_i on e.g. rms-values of velocity and temperature fluctuations and on their energy spectra for X_i = 4 to 8, but no significant differences for X_i = 8 and greater. Thus X_i = 8 is considered adequate for our purposes.

Considering the influence of the problem time t_{max} over which the simulation for sodium is performed, Tab. 2, we found statistically stationary flow after t = 200 to 300, see e.g. the rms-value of the temperature fluctuations in Fig. 1. Some small long wave random oscillations occured in the flow

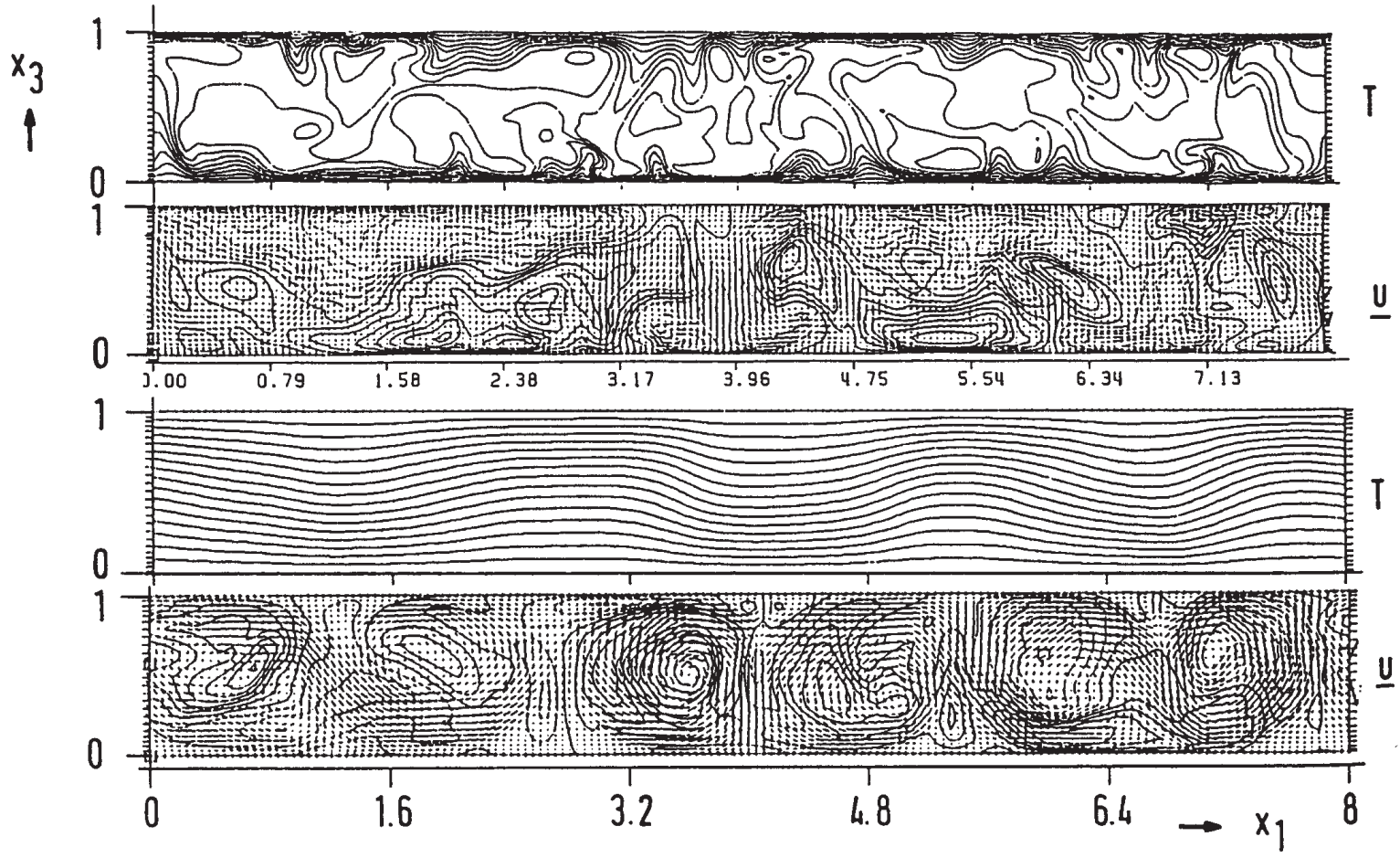

Figure 2. Vertical sections through instantaneous temperature and velocity fields at any position and time for Pr = 0.71 (top) and Pr = 0.006 (bottom)

field with periods around 20 to 150, as was similarly observed in experiments [8]. The extremely long problem time was chosen to ensure at least in one simulation that at this small Rayleigh number no relaminarisation or regular time periodic flow will occur. In the future we may simulate shorter time intervals again.

Analysis of turbulent momentum transfer

Before we study some terms of the k-ε-g heat transfer model we present the results for the vertical profiles of the kinetic turbulence energy $k = \overline{u'_i{}^2}/2$ and its dissipation ε which were analysed from the simulation results using their analytical definitions. The profiles for k, Fig. 3, compare for both fluids quite well in the near wall range. The k boundary layer is somewhat thicker for sodium, despite of a larger Grashof number. In the inner part of the channel the sodium flow gives only one maximum in the middle of the channel as it occurs with air at much smaller Grashof numbers.

The analytical form of the complete conservation equation for k in Rayleigh-Benard convection is

$$\partial k/\partial t = -\,Gr/Re_o^2\ \overline{\underline{u}'T'} - \mathrm{div}\,[\overline{\underline{u}'E} + \overline{\underline{u}'p'}] + \nu\,\mathrm{div\,grad}\ k - \varepsilon$$

prod. turb.diff. visc. diff.

with $Re_o = u_o D/\nu$ and

$$\varepsilon = \nu\,(\overline{(\mathrm{rot}\,u')^2} + 2\,\overline{\mathrm{div}\,(u'\,\mathrm{grad}\,u')}).$$

Statistical analysis of the production, diffusion, and dissipation terms of this equation results in only small differences in the dissipation of k, Fig. 4. The dissipation of k is governed by the smallest scales in the velocity field which are very similar according to Fig. 2. The production term is proportional to the turbulent heat flux, and thus shows considerable differences between both cases. In air most heat is transfered upwards by convection whereas with sodium a relatively small amount of heat is transfered by convection. The form of the vertical profiles is consistent with the large differences in the thicknes-

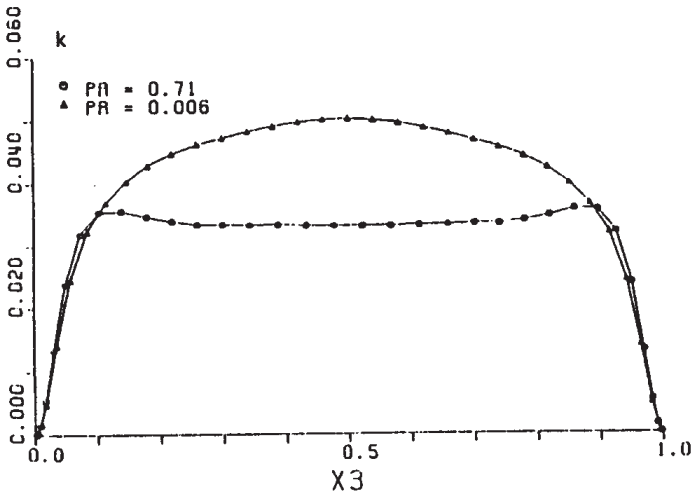

Figure 3. Vertical profile of the kinetic turbulence energy k

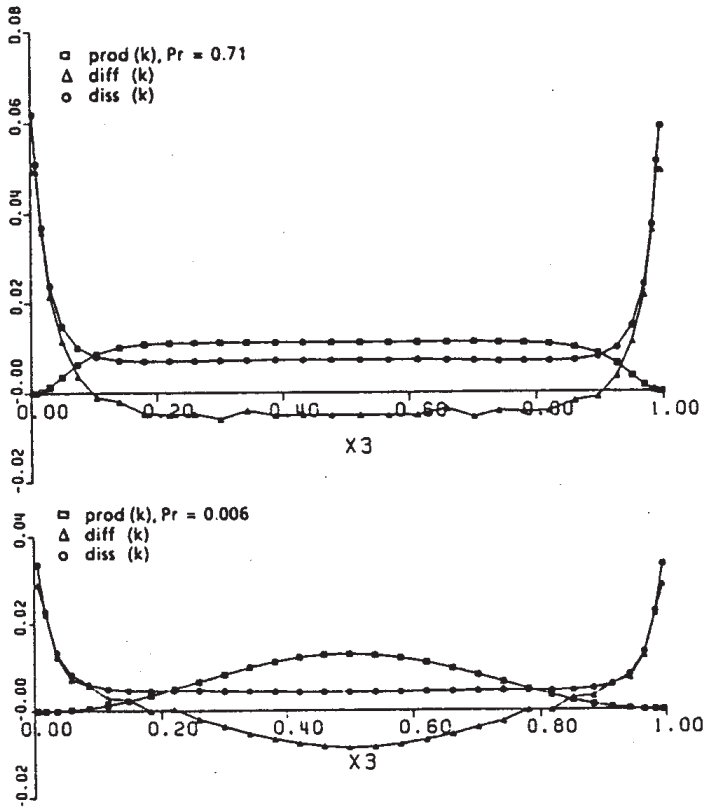

Figure 4. Terms of the k-equation for Pr = 0.71 (top) and Pr = 0.006 (bottom)

ses of the thermal boundary layers. For Pr = 0.71 the thickness of the thermal boundary layer is about 0.1·D whereas for Pr = 0.006 both boundary layers meet at half height. As a consequence, the term of the molecular plus turbulent diffusion which is responsible for the vertical redistribution of k, looks very different in both cases. Thus, closure assumptions for the turbulent diffusion will have to account for the influences of the molecular Prandtl number.

The similarity at small scales obvious from both dissipation profiles does not help very much in modelling this term. This is indicated by analysing

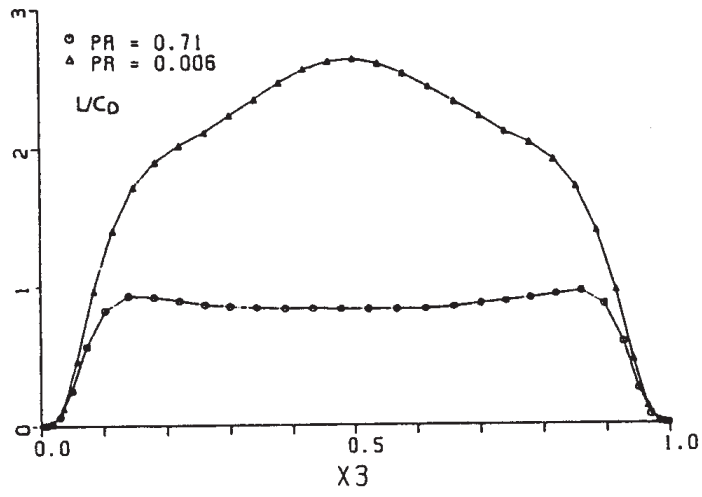

Figure 5. Length scale L/C_D of Rotta's dissipation model $\varepsilon = C_D\,k^{3/2}/L$

$$L/C_D = k^{3/2}/\varepsilon,$$

Fig. 5, which is the Rotta model for the dissipation in a one-equation k model at large turbulence levels [15]. This length scale strongly depends on Pr mainly because of the differences in the k profile. For sodium a much larger value for L/C_D is predicted. This length is assumed to give a measure for the size of the large flow structures; here this qualitatively agrees with the above mentioned existence of roll-like structures with an axial extent of 6 to 8. In the simulation with air such large horizontal roll-like structures do not exist. There we find spoke pattern like structures forming highly irregular cells with typical diameters of about 3.4 [13].

Analysis of turbulent heat transfer

The analysed vertical profile of the time mean temperature which should be the result of a turbulent heat transfer model is given in Fig. 6. For air the well known behaviour is found with thin thermal boundary layers corresponding to a Nusselt number of 6.26, and an isothermal core. For sodium at this Rayleigh number a roughly linear temperature profile is developed which means, the convection is, in accordance with the small value of the Nusselt number, of negligible influence on heat transfer.

The analysis of the turbulent Prandtl number $Pr_t = \nu_t/a_t$, which is often used to calculate heat transfer with the k-ε model, is not possible in a simple manner. The turbulent eddy diffusivity

$$\nu_{tj} = -\overline{u'_3 u'_j}/(\partial \overline{u_j}/\partial x_3),$$

is not well defined in Rayleigh-Bénard convection because the time mean vertical momentum fluxes as well as the time mean horizontal velocities $\overline{u_j}$, j = 1,2, are zero. To circumvent this problem we assume the validity of the standard k-ε model [15],

$$\nu_t = C_\mu k^2/\varepsilon,$$

with $C_\mu = 0.09$, and calculate ν_t from the simulation results for k and ε. The turbulent eddy conductivity

$$a_t = -\overline{u'_3 T'}/(\partial \overline{T}/\partial x_3)$$

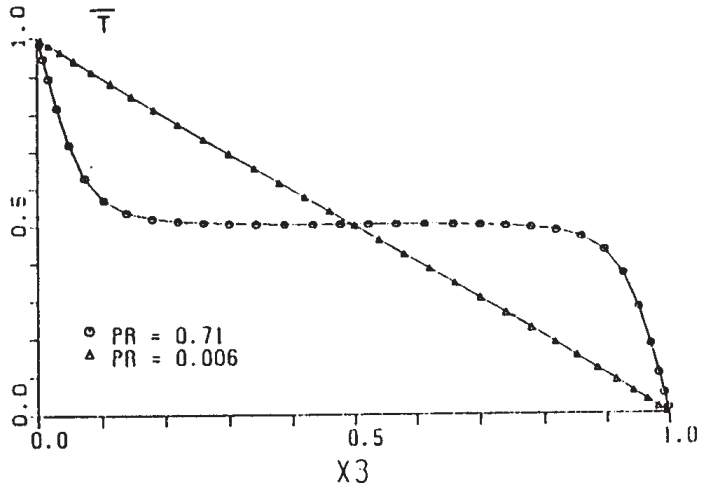

Figure 6. Vertical time mean temperature profile

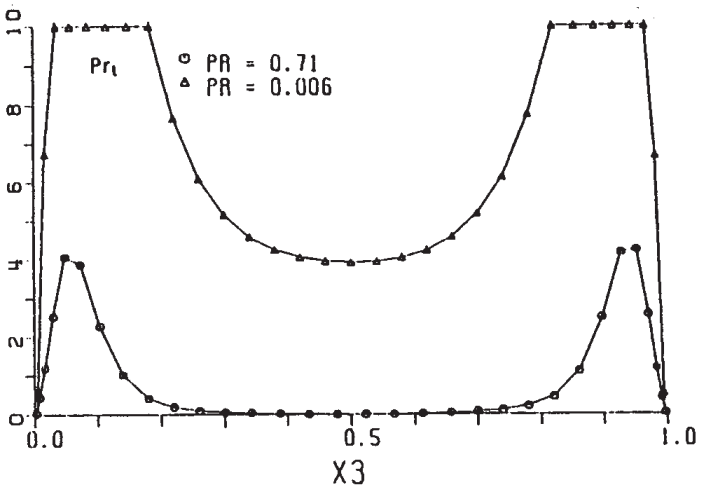

Figure 7. Turbulent Prandtl number analysed by using the expression for ν_t from the standard k-ε model. ($Pr_t < 10$ enforced in this plot)

is well defined and can be analysed directly from the simulation results. The values for Pr_t gained on this way show strong vertical variations, Fig. 7. Especially in the inner part of the channel where the assumption for ν_t should be valid we find values which do not coincide with values used practically. The reason for Pr_t to become zero locally with air is its definition as thermal gradient diffusion. The air flow has an isothermal core, Fig. 6, which gives $Pr_t = 0$, whereas in practical calculations no gradient model will give an isothermal core. Thus gradient diffusion should not be assumed in this type of flow. For sodium at this small Rayleigh number the problem does not occur and Pr_t is larger than one as it is expected.

The problem of using uncertain turbulent Prandtl numbers is circumvented in models using combinations of k-ε models, Algebraic Stress Models, and the $g = \overline{T'^2}/2$ equation [15]. Thus we need the distribution of g and of the terms in the conservation equation of g. This equation in Rayleigh-Benard convection reduces to:

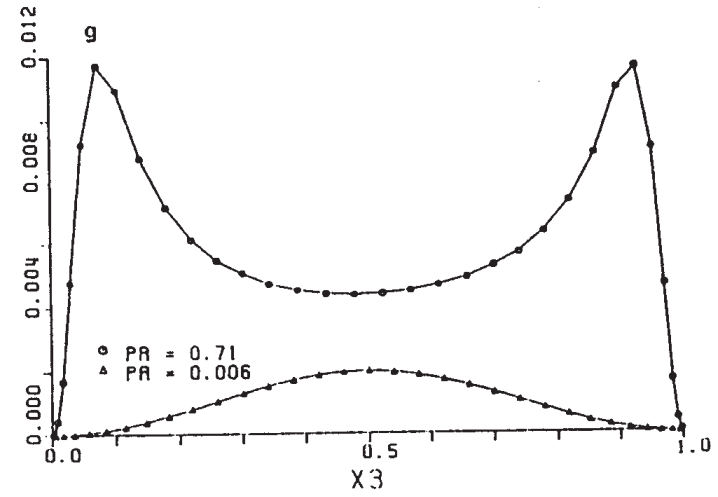

Figure 8. Vertical profile of time mean temperature variances $g = \overline{T'^2}/2$

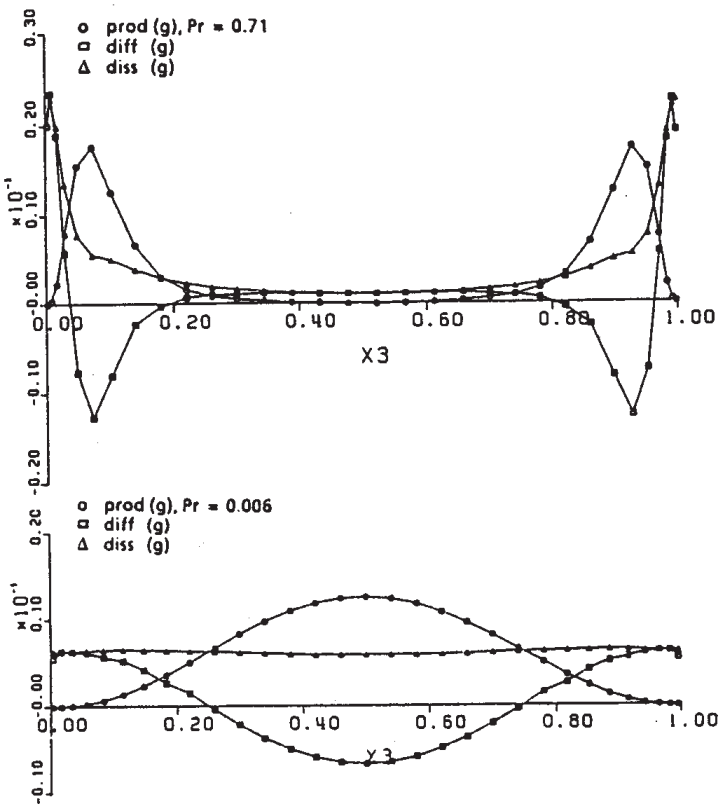

Figure 9. Terms of the g-equation.
Prod = $-\overline{u'_3 T'}\,\partial\overline{T}/\partial x_3$; Diff = $-\partial\,\overline{u'_3\, g}/\partial x_3 + a\partial^2 g/\partial x^2_3$; Diss = $a\,\overline{(\partial T'/\partial x_i)^2}$.

$$\partial g/\partial t = -\overline{\underline{u}'T'}\,\mathrm{grad}\,\overline{T} - \mathrm{div}\,\overline{\underline{u}'g} + a\,\mathrm{div}\,\mathrm{grad}\,g - a\,\overline{(\mathrm{rot}\,T')^2}$$

prod. turb.diff. therm.diff. dissip.

The vertical profile of g for air has two maxima, each near the edge of the thermal boundary layer, Fig. 8. For sodium the values are much smaller and only one maximum occurs, also near the edge of the thermal boundary layer.

Statistical analysis of the analytical terms of the g equation results in a production term which is for both simulations very similar to the g profiles, Fig. 9. The dissipation ε_g of g looks at the larger Prandtl number comparable to that of k, but it is roughly constant for the sodium case. As a consequence the diffusion term for g has also two distinct minima at the edges of the thermal boundary layers at Pr = 0.71 and a wide relative maximum in the middle of the channel. The latter feature cannot be found at Pr = 0.006 because of the relative dominance of conduction over convection. Comparing the results for both fluids we cannot separate the influences of Ra and Pr. Besides, the diffusion terms in Fig. 4 and 9 are very much suited to judge on the accuracy of the analysis, of the simulation, and of the status of development of the flow. This term, which is analysed indepently from the other ones, has always to balance the differences between the two other curves.

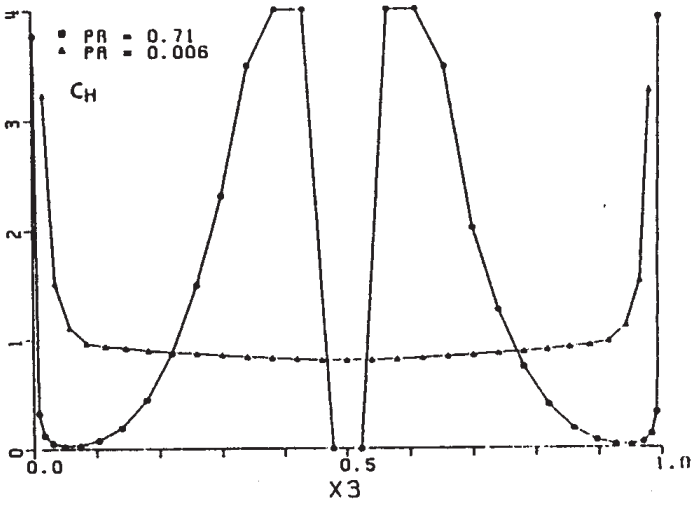

Figure 10. Coefficient C_H of Meroney's k-ε-g heat flux model.

With the results given up to now the coefficient C_H in one of the existing k-ε-g models [16],

$$a_t = C_H\, k\, g / \varepsilon_g$$

can be calculated, Fig. 10. For air C_H shows strong vertical variations which are due to the definition of a_t as an effective conductivity in a gradient model for the turbulent heat flux. Again the isothermal core and some local temperature inversion (perhaps caused by insufficient time averaging) leads to abrupt changes in C_H and thus shows the problem with gradient models. For sodium a sufficiently smooth distribution of C_H is found, but in the relevant region, that is within the thermal boundary layers, the value of C_H is much larger than the one of $C_H \approx 0.03$ - 0.1 found with air and of $C_H = 0.1$ used practically in [16]. Thus, this model needs careful consideration of the influence of Ra and Pr on C_H.

Closure assumptions are required to solve the g equation numerically. One of the models for the dissipation ε_g relates this to ε by a time scale ratio R [15]:

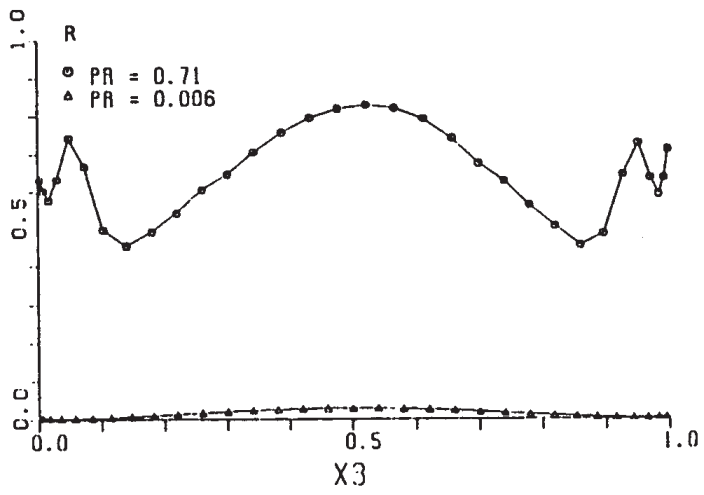

Figure 11. Time scale ratio R of the model for the dissipation ε_g.

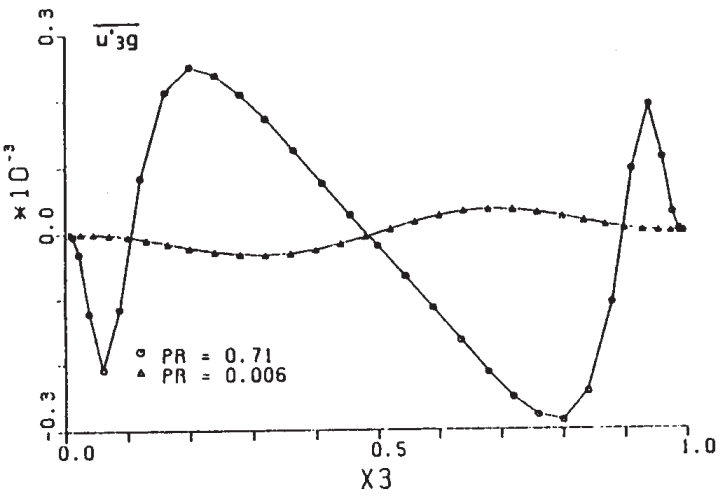

Figure 12. Triple correlation $\overline{u'_3\, g}$ in the diffusion term of the g quation.

$$\varepsilon_g = \varepsilon\, g / (k\, R).$$

The value of R varies for air between 0.45 and 0.7, Fig. 11. The complicated vertical variation is due to the different locations at which the maxima in k, g, and ε occur. In calculations using this model often constant values between 0.5 and 1 are used. These values obviously do not hold for low Rayleigh number convection in sodium because the time scales of the temperature fields for air and sodium are very different.

In choosing a closure model for the triple correlation $\overline{u'_3\, g}$, Fig. 12, from the turbulent diffusion of g we have again to consider that models containing mean shear terms cannot be used here. A possible alternative is

$$\overline{u'_3 g} = -C'_T\, k^2/\varepsilon\, \partial g/\partial x_3,$$

[15]. The value of the analysed coefficient C'_T for air varies strongly with x_3 and shows large peaks near the walls, Fig. 13; this means the model gives no adequate results for this type of convection. In addition we find no distinct regions in which C'_T takes a

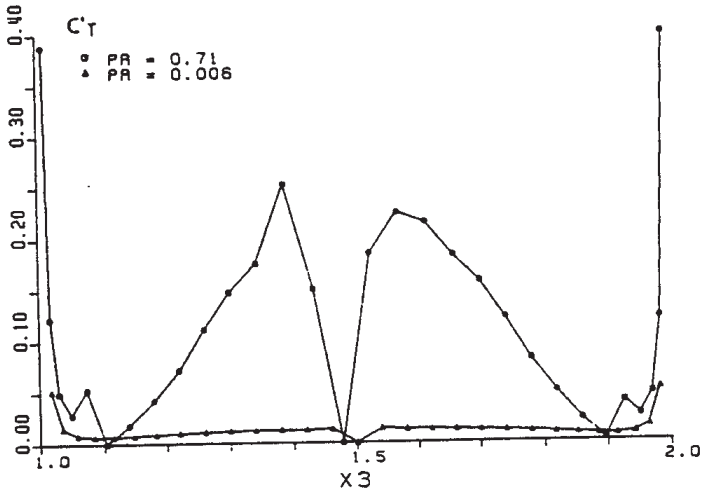

Figure 13. Coefficient C'_T used in Spalding's model for $\overline{u'_3\, g}$.

locally constant value of 0.13 which is the recommended number for this coefficient. The results for sodium do not show this problem; the Rayleigh number is too small to give such strong variations in the channel. The model deficiency found is not of importance at low Rayleigh numbers in liquid metals because the molecular diffusion dominates the turbulent diffusion of g.

CONCLUSIONS

The method of direct numerical simulation was used to produce a data base for Rayleigh-Bénard convection in air and sodium at about comparable Grashof numbers at small turbulence levels. The results were used to investigate the flow structure in liquid metal convection and to give first values for the large scale structures of the flow. The small scale structures in the velocity fields of both fluids look very similar in accordance with the Grashof number similarity.

Statistical analysis was performed for the turbulent heat flux models, for terms in the k and g equation, and for some model assumptions in a standard k-ε-g model. The widely used turbulent Prandtl number concept can not give accurate results. It will enforce non-isothermal cores. In addition Pr_t strongly depends on the molecular Prandtl number. The dissipation of kinetic energy is in both cases comparable. Nevertheless models available suffer from influences by the Prandtl number. The other models considered, especially those for the dissipation of temperature variances g and for its turbulent diffusion, depend strongly in an up to now not analysed manner on the Rayleigh and Prandtl numbers. The diffusion model seems not to be adequate to the physical problem considered. The results for the model coefficients may suffer from considering a standard k-ε model which has no special model extensions to incorporate effects of near wall damping, of buoyancy contributions, or of low Reynolds numbers. Thus the given coefficients for air are valid only apart from walls, and those for sodium should be considered only as tentative results because the "turbulence level" in the scalar field is very small. In future work we will try to circumvent these discussed limitations in our analysis and will also try to compare our results with those of standard k-ε codes. Anyway, it is evident from the available results that all molecular thermal diffusion type terms have to be included, e.g. in the g equation, in a model when it shall be used with liquid metals and that low Reynolds number extensions have to be used to treat more accurately the wall proximity.

REFERENCES

[1] K. SATOH, H. MIYAKOSHI, "Study of decay heat removal by natural circulation," *Proc. NURETH-4*, pp. 378-383 (1989).

[2] H. HOFFMANN, H. KAMIDE, K. MARTEN, H. OHSHIMA, D. WEINBERG, "Investigations on the transition from forced to natural convection for the pool type EFR in the 3d RAMONA model," *Int. Conf. on Fast Reactors and Related Fuel Cycles*, Kyoto, Oct. 28 - Nov. 1, (1991).

[3] H. NINOKATA, "Advances in computer simulation of fast breeder reactor thermalhydraulics," *Proc. SNA '90*, pp. 80-85 (1990).

[4] H.A. BORGWALDT, "CRESOR, a robust vectorized Poisson solver implemented in the COMMIX-2(V) thermal-hydraulics code," *Proc. SNA '90*, pp. 346-351 (1990).

[5] S.P. LAWRENCE, "Turbulence modelling in naturally convecting fluids," *Culham Lab., CLM-R292*, Sept. (1989).

[6] L. DAVIDSON, "Calculation of the turbulent buoyancy-driven flow in a rectangular cavity," *Num. Heat Trans.* A, Vol. 18, pp. 129-147 (1990).

[7] D. SUCKOW, "Experimentelle Untersuchungen turbulenter Mischkonvektion im Nachlauf einer punktförmigen Wärmequelle," *Dr. thesis*, Univ. Karlsruhe, to be published

[8] V. KEK, "Bénard Konvektion in flüssigen Natriumschichten," *Dr.-thesis*, Univ. Karlsruhe, KfK 4611, (1989).

[9] G. GRÖTZBACH, "Direct numerical and large eddy simulation of turbulent channel flows," *Encyclopedia of Fluid Mechanics*, Gulf Publ., Houston, Vol. 6, pp. 1337-1391 (1987).

[10] M. WÖRNER, G. GRÖTZBACH, "Analysis of semi-implicit time integration schemes for direct numerical simulation of turbulent convection in liquid metals," *Proc. GAMM 1991, Lausanne, to appear in Notes on Numerical Fluid Mechanics*, Vieweg, Braunschweig.

[11] G. GRÖTZBACH, "Spatial resolution requirements for direct numerical simulation of the Rayleigh-Bénard convection," *J. Comp. Phys. 49*, pp. 241-264 (1983).

[12] G. GRÖTZBACH, "Numerical simulation of oscillatory convection in low Prandtl number fluids with the TURBIT code," *Notes on Num. Fl. Mech.*, Vol. 27, pp. 57-64 (1990).

[13] G. GRÖTZBACH, "Simulation of turbulent flow and heat transfer for selected problems of nuclear thermal-hydraulics," *Proc. SNA '90*, pp. 29-35 (1990).

[14] F.H. BUSSE, "Non-linear properties of thermal convection," *Rep. Prog. Phys.*, Vol. 41, pp. 1929-1967 (1978).

[15] W. RODI, "Turbulence models and their aplication in hydraulics - A state of the art review," *IAHR-publication*, Delft (1980).

[16] R.N. MERONEY, "An algebraic stress model for stratified turbulent shear flows," *Comp. and Fluids*, Vol. 4, pp. 93-107 (1976).